Complete remission in a patient with widely metastatic HER2-amplified pancreatic adenocarcinoma following multimodal therapy informed by tumor sequencing and organoid profiling

Daniel A King[1], Amber R Smith[2], Gino Pineda[3], Michitaka Nakano[4], Flavia Michelini[5], S. Peter Goedegebuure[6], Sheeno Thyparambil[7], Wei-Li Liao[7], Aaron McCormick[4], Jihang Ju[4], Michele Cioffi[8], Xiuli Zhang[6], Jasreet Hundal[6], Malachi Griffith[9], Carla Grandori[10], Maddy Pollastro[10], Rachele Rosati[10], Astrid Margossian[10], Payel Chatterjee[10], Trevor Ainge[10], Marta Flory[11], Paolo Ocampo[12], Lee-may Chen[13], George A Poultsides[14], Ari D Baron[15], Daniel T Chang[16], Joseph M Herman[17], William E Gillanders[6], Haeseong Park[18], William A Hoos[19], Mike Nichols[20], George A Fisher[3], Calvin J Kuo[3]*

1. Northwell Health Cancer Institute and Feinstein Institute of Research, Lake Success, NY
2. Xilis Corporation, Durham, NC
3. Stanford Cancer Institute, Stanford, CA
4. Department of Medicine, Divisions of Heamatology and Oncology, Stanford University School of Medicine, Stanford, CA 94305
5. Memorial Sloan Kettering Cancer Center, NY, NY
6. Department of Surgery, Washington University School of Medicine in St Louis
7. Mprobe, Inc, Rockville, MD
8. Cornell University, School of Medicine, NY, NY
9. Department of Medicine, Washington University School of Medicine
10. SEngine Precision Medicine, Seattle, WA
11. Department of Radiology, Stanford University, CA
12. Personalized Healthcare, Genentech, Inc., South San Francisco, CA, 94080
13. Department of Gynecologic Oncology, University of California at San Francisco, San Francisco, CA
14. Department of Surgery, Section of Surgical Oncology, Stanford University, Stanford, CA, USA
15. Division of Hematology Oncology, California Pacific Medical Center
16. Department of Radiation Oncology, Stanford Cancer Institute, Stanford, CA
17. Department of Radiation Oncology and Northwell Health Cancer Institute, Lake Success, NY
18. Department of Medicine, Division of Oncology, Washington University School of Medicine in St Louis
19. xCures Inc, Oakland, CA
20. Independent Clinician, Saratoga, CA

* Corresponding Author

Abstract

Here, we demonstrate a complete clinical response achieved in a patient with HER2+ metastatic pancreatic ductal adenocarcinoma to a coordinated barrage of anti-HER2, personalized vaccine and checkpoint inhibition immunotherapy, radiation, and chemotherapy. Comprehensive organoid profiling with drug sensitivity screening and drug testing suggested a vulnerability to anti-HER2 directed therapy, facilitating personalized treatment selection for our patient, which contributed to her clinical benefit. Immune response monitoring following personalized vaccine, radiation and checkpoint inhibition showed a sustained increase in neoantigen specific T cell response.

Introduction

Pancreatic ductal adenocarcinoma (PDAC) remains among the deadliest of all human cancers[1], compelling discovery of new predictive biomarkers and tailored therapies for this refractory disease. HER2 is a cell membrane receptor tyrosine kinase whose overexpression precipitates oncogenesis in several cancer types and is actively explored as a therapeutic target[2].

HER2 overexpression in PDAC is uncommon, occurring in 2.1% of patients, of which 1.5% exhibit grade 3+ immunohistochemistry (IHC) positivity. The remaining 0.6% are IHC grade 2+ with amplification confirmed by *fluorescent in situ hybridization* (FISH)[3,4]. The role of HER2 as a prognostic and predictive biomarker in PDAC is controversial. While early studies indicated that HER2 amplification in PDAC may be a poor prognostic feature[5,6], these findings were confounded by an overestimation of HER2 expression[3,7]. In contrast, both a recent large study[4] and separate meta-analysis that measured HER2 amplification by FISH[8], did not observe significant association between HER2 amplification and survival in PDAC. These data suggest that HER2 is not strongly prognostic in PDAC. Regarding HER2 as a biomarker of response to anti-HER2 directed therapy in PDAC, in vitro and in vivo animal models have indicated dose-dependent and HER2-expression-correlated survival improvements[9–12]. However, to date, human trials evaluating trastuzumab in combination with gemcitabine[13], capecitabine[14], or gemcitabine and erlotinib[15], have shown median overall survival of 6.9-7.9 months, consistent with lackluster clinical benefit compared to standard of care therapy. Notably, these HER2-unselected PDAC trials measured a higher frequency of HER2+ tumors (11%-58%) compared to the ~2% population rate as assessed by modern standards, suggesting inclusion of patients without true HER2 positivity, potentially hindering validity of these studies[16]. In other GI malignancies, especially gastroesophageal cancer, HER2 is a strong predictive biomarker[17,18].

Several immune-based treatments have been studied for PDAC, including peptide vaccine, recombinant vaccine, and irradiated whole tumor cell vaccines[19], adoptive cell transfer, CAR-T therapy and checkpoint inhibitors[20]. These interventions have had minimal efficacy[21]. For example, a recent study of 50 treatment-naïve patients with advanced PDAC treated with combination gemcitabine, nab-paclitaxel, and nivolumab exhibited a median overall survival of only 9.9 months[22]. Several ongoing phase I or II studies using checkpoint inhibition combined with chemotherapy, radiotherapy, or vaccine therapy such as GVAX and personalized mRNA vaccines, are underway in PDAC[21,23,24]. In gastroesophageal cancer, combination trastuzumab and pembrolizumab recently received FDA approval for first-line treatment based on a response rate of 74%, including an 11% complete response rate[25]. However, in PDAC, combination anti-HER2 therapy with immune checkpoint inhibition has not been reported.

Organoid modeling is an in vitro method that allows dissociated primary tissue, including tumors, to be propagated in three-dimensional tissue culture onto a physical scaffold (matrix) [26–28]. Patient-derived organoids can be generated from tumor biopsies by cultivation in submerged ECM, such as Matrigel/BME, or can be grown in air-liquid interface (ALI) culture by embedding freshly minced tissue in a collagen bed[29]. Gene expression profiling of organoids can predict tumor responses to therapy[30] and in vitro testing of drug panels can permit personalized drug screening[31]. In this study, organoids were generated from a patient's tumor and suggested response to anti-HER2 therapy.

We report a patient with PDAC and HER2 overexpression whom we treated with anti-HER2, immunotherapy, and radiation (RT) combination treatment. In our patient, multiple lines of evidence indicated a high-copy HER2 amplification, raising speculation that her tumor might be driven by HER2 over-activity and thus sensitive to HER2 inhibition. The choice of an anti-HER2 treatment component was motivated by prior studies showing high responses in HER2+ gastric cancer[32], and organoid modeling experiments predicting sensitivity to anti-HER2 inhibition. On progression of disease, recent advances in anti-HER2 therapy combined with RT and immunotherapy[25] motivated the use of immune-based treatments, which included checkpoint inhibition and vaccine therapy. Following combined therapy, the patient achieved a durable complete clinical response. Overall, these findings suggest combining anti-HER2 therapy with RT and immunotherapy may be effective for the PDAC patient population with HER2 overexpression.

Case Report

A previously healthy woman in her 50s presented with an elevated CA-125 level, which had been ordered by her primary care physician as part of a quarterly tumor marker screening panel. On

questioning, the patient endorsed abdominal discomfort. An initial pelvic ultrasound observed a large adnexal mass concerning for suspected ovarian cancer. MRI of the abdomen and pelvis identified a 6.3 cm left cystic ovarian mass, a 3.2 cm right ovarian mass, a 3.9 cm pancreatic mass, and at least two liver lesions. In August of 2017, she underwent a hysterectomy, bilateral salpingo-oophorectomy, and infragastric omentectomy. Surgical pathology demonstrated a 10-cm conglomerative omental metastatic mass and bilateral ovarian involvement of a moderately differentiated mucinous adenocarcinoma. Immunohistochemistry staining was notable for CD7 positive, CD20 weak, PAX8 negative, WT1 negative, and DPC4 absence. Histologically the tumor cells contained a pale cytoplasm with mucinous features, strongly suggestive of a metastasis from a pancreaticobiliary primary site rather than an ovarian primary. CT imaging three weeks following surgery identified both an unresected distal pancreatic body mass and concomitant metastatic disease in the liver and hemidiaphragm. Germline genetics evaluation with the Invitae Multi-Cancer Panel identified no pathogenic mutations. Tumor mutational profiling results were pending at the time that systemic therapy was initiated.

In September 2017, the patient began treatment with gemcitabine and protein-bound paclitaxel, combined with indoximod, an investigational immunometabolic agent targeting the IDO pathway, as part of a phase I/II clinical trial (Figure 1)[33,34]. The patient responded well to therapy initially. Pre-treatment CA 19-9 was 17,784 U/mL. Following 10 months of therapy, CA 19-9 reached a nadir of 36 u/mL and a clinical partial response was observed. At that time, her disease burden consisted of a 1.2 cm pancreatic tail mass, a 1.1 cm lesion in the liver, and subcentimeter nodules in the lungs, liver, and peritoneum. Tumor profiling results from her initial resection were then obtained which indicated HER2 overexpression and pathogenic DNA mutations (Table 1). Four months later, her disease burden remained stable except for a single peritoneal lesion in the hepatorenal recess, which had grown to 3.1 cm. Given that the metastasis appeared isolated, and that surgery was considered low risk, the hepatorenal recess lesion was resected in November of 2018. Consistent with her initial resection, the peritoneal lesion exhibited HER2 amplification (Table 1). The tissue showed intact expression of mismatch repair proteins. She then received trastuzumab and pertuzumab on the TAPUR trial[35].

On this dual anti-HER2 therapy, the patient's disease remained stable for 9 months but due to rising CA 19-9 levels she opted to pursue investigational vaccine therapy while continuing trastuzumab and pertuzumab off-trial (Figure 1). In January of 2020, the patient initiated treatment with an investigational neoantigen recombinant DNA vaccine being studied in a phase I trial sponsored by Washington University School of Medicine[36,37], but as the trial was fully enrolled, the vaccine was provided for compassionate use off-trial. In March 2020, a PET scan showed

interval growth of the primary pancreatic lesion in addition to two slow growing ~1 cm lung lesions in the setting of otherwise stable disease. Multi-disciplinary review among collaborators brought together by the Canopy Cancer Collective pancreatic cancer learning network of recent data suggesting efficacy of concurrent checkpoint inhibition with radiation[38] and oligometastatic disease[39] influenced the decision to initiate stereotactic radiation (SBRT) for her pancreatic tumor (40 Gy in 5 fractions) and to the 2 PET avid foci in her bilateral lungs suspected to be metastatic (25 Gy in 1 fraction to LUL and 40 Gy in 4 fractions to the RLL). Imaging and CA 19-9 were consistent with a partial response to treatment. Following completion of radiotherapy, the patient commenced treatment with ipilimumab and shortly thereafter in combination with nivolumab, however the patient discontinued checkpoint inhibition therapy after approximately 6 months due to signs of pneumonitis and acute kidney injury. She was briefly prescribed hydroxychloroquine, but this was discontinued due to nausea and indigestion. Off-label trastuzumab deruxtecan was then added in July 2020 to her ongoing combination immunotherapy with nivolumab and the monthly personalized vaccine. Her CA 19-9 decreased below the upper limit of normal in August 2020. From October 2020, further targeted therapy was held, and only monthly personalized vaccine therapy was continued. By 2021, following approximately four months of combination of targeted anti-HER2 treatment and immunotherapy, imaging showed no evidence of recurrent or metastatic disease. In April 2021, her CA 19-9 measured 4.7, her nadir throughout treatment. As of October 2021, the patient has remained without evidence of disease, asymptomatic and active.

Molecular Analyses & Organoid Profiling

First-line gemcitabine-based treatment was initiated prior to availability of tumor mutational profiling data, which subsequently showed a *KRAS* G12D mutation, HER2 amplification, PD-L1 positivity (2% of tumor cells), and other abnormalities (Table 1). Thereafter, molecular profiling of the patient's longitudinal tumor samples and CLIA-grade drug testing of the tissue-derived organoid informed the selection for the targeted and immunooncology therapies she received.

Upon development of a new site of disease in the hepatorenal recess in November 2018, and prior to initiation of therapy, the tissue was biopsied and subjected to whole exome sequencing, RNA sequencing, and organoid generation (Figure 2). Organoids were generated using the air-liquid interface (ALI) culture method[29] and passaged and maintained using conventional submerged medium culture methods in Cultrex® Reduced Growth Factor Basement Membrane Matrix, Type 2 (BME-2) as described[30] for subsequent characterization and drug testing. Histological characterization of the generated organoids correlated with original tumor tissue, and the organoid line expressed HER2, assessed by IHC. The whole exome and RNA

sequencing results of the organoid matched those from the original surgical sample and the high-copy HER2 amplification was preserved (Table 1). The magnitude of organoid HER2 amplification was substantial, reported as more than 20 copies. Following this molecular validation, the organoid sample was sent to several collaborating institutions for further molecular analysis (Figure 3).

CLIA-grade organoid drug sensitivity testing by SEngine demonstrated that anti-HER2 therapy had the highest predicted potency of 39 tested drugs (Supplementary Materials). Organoid drug testing by Memorial Sloan Kettering Cancer Center (MSKCC) also demonstrated sensitivity to anti-HER2 therapy: following a 6-day treatment to the anti-HER2 antibody drug conjugate trastuzumab deruxtecan (T-DxD), approximately 70% of cells died, an effect driven mostly by apoptotic cell death, whereas nearly 100% of cells exposed only to vehicle control remained viable (Figure 3A-C and Supplementary Materials). Xenograft transplantation into immunodeficient mice was attempted for this organoid sample and was not successful; however, an *in vivo* xenograft using organoid tissue from a different patient with PDAC harboring a 4-fold *HER2* amplification and *KRAS* G12D mutation was viable and showed marked reduction in tumor volume after exposure to T-Dxd compared to control (Figure 3D). Lastly, quantitative HER2 expression profiling of organoids using mass spectrometry conducted by mProbe demonstrated a markedly elevated HER2 expression level, above the threshold of predictive sensitivity to anti-HER2 directed therapy[40] (Table 1). Based on these findings the patient was enrolled on a trial using anti-HER2 directed therapy using trastuzumab and pertuzumab, and her disease remained stable for approximately nine months.

Subsequent follow-up discovered local recurrence in the pancreas as well as clinically diagnosed oligometastatic pulmonary metastases. In January 2020, she began monthly treatments with a personalized DNA vaccine[36] (Figure 4). A list of the neoantigens incorporated into the vaccine, the mutant and wildtype amino acid sequences, and predicted binding is included in Supplementary Table 2. In March of 2020, SBRT, using 40 Gy over 5 fractions, was delivered. The patient experienced a rapid molecular and radiographic response to this combined radio-immunotherapy. During the fiducial placement for radiation, the pancreatic body primary lesion was biopsied, from which attempted organoid generation was not successful, possibly due to poor tumor viability on-treatment; however, mutation profiling with Next Generation Sequencing (NGS) and RNA sequencing by Tempus on that tissue confirmed continued high-copy HER2 amplification with a > 99.7% rank among the PDAC population assessed by Tempus. This motivated incorporation of continued anti-HER2 directed therapy using trastuzumab deruxtecan (T-DXd), consisting of the monoclonal antibody trastuzumab linked to the topoisomerase inhibitor

deruxtecan. Her response continued to deepen on multi-modal therapy, achieving a molecular and radiographic complete response.

To assess whether the dramatic responses achieved were at least partially attributable to the vaccine, functional studies of immune-driven tumor suppression were performed, which demonstrated that the neoantigen DNA vaccine induced CD4 and CD8 neoantigen-specific T cell responses (Figure 4). IFNγ ELISpot assay performed after in vitro culture of PBMCs collected pre- and post-vaccination (week 17) with pooled neoantigens indicated that the neoantigen DNA vaccine induced robust T cell responses against three neoantigens FOXP3 (p.A349T), FAM129C (p.G520R), and ANK2 (p.R2714H) (Figs 4B, C, and F). Further study by intracellular cytokine staining demonstrated that ANK2-specific CD4 (9.05%) and CD8 (23.1%) T cell responses were induced after stimulation of PBMC with ANK2 (Figs. 1D and 1E). The response to FOXP3, FAM129C, and ANK2 persisted over time (Fig. 1F). Of note, the bars in Fig. 1F indicate the average response to FOXP3, FAM129C, and ANK2. None of the other antigens induced a consistent response over time.

The patient's blood samples continue to be assessed for circulating disease and she remains in clinical and molecular remission.

Discussion

This report highlights the case of a patient with metastatic pancreatic cancer and HER2-amplification, who achieved a complete response following multiple lines of targeted and immune-based therapies. Initially, she underwent surgical debulking for suspected ovarian cancer, whereas this procedure is generally reserved for symptomatic or chemo-refractory disease for PDAC. Subsequently, she underwent gemcitabine-based treatment, anti-HER2 therapy, and then third-line combination therapy with an HER2-directed antibody conjugate, radiation, checkpoint, and personalized vaccine therapy. Remarkably, following combination therapy, the patient has achieved a deep and durable remission.

Complete responses are rarely observed in PDAC, representing 0.2% (1 of 431) of patients who received first-line FOLFIRINOX on trial[41], 0.6% (1 of 171) of patients treated with first-line gemcitabine and nab-paclitaxel on trial[42], and 0.0% (0 of 212) of patients who received nano-liposomal irinotecan following progression on gemcitabine-based therapy[43]. In a trial of patients with germline BRCA deficiency, 2% (2 of 92) of PDAC patients achieved a complete response on olaparib[44]. Thus, the observation that a complete and durable response was achieved in the third line setting prompts speculation that the patient's disease biology, treatment regimens, or combination may be explanatory.

The patient's tumor was notable for HER2 amplification. Multiple lines of evidence resulting from our organoid studies indicated potent sensitivity to anti-HER2 directed therapy. Her disease stability of dual HER2-directed therapy, lasting 9 months, compared to a median expected progression free survival of 4.4 months in the second-line setting[45], and deep remission achieved on trastuzumab deruxtecan were coincident, suggesting a mechanistic underpinning. As one explanation, this patient had an exceptionally high HER2 copy number state, perhaps suggesting a component of oncogene addiction driven by a quantitative relationship between HER2 amplification and response in PDAC. Accordingly, prior literature in gastric cancer[40], breast cancer with trastuzumab[46] and trastuzumab deruxtecan[47] support a positive correlation between HER2 gene copy number and response to anti-HER2 therapy. Conversely, loss of HER2 expression has been observed as a mechanism of resistance following anti-HER2 therapy in gastric cancer[48,49]. Notably, molecular profiling of the patient's relapsed tumor showed persistent high-copy HER2 amplification following trastuzumab and pertuzumab which informed subsequent anti-HER2 therapy.

The deepest measured responses achieved, as assessed by a logarithmic drop in CA 19-9 and reduction in volumetric tumor burden, occurred at the initiation of therapy, and during radiation and immunotherapy. While it is possible that the response to radiation and immunotherapy would have been sustained and led to a complete response on their own, anti-HER2 therapy appeared to contribute to and may have potentiated the effect of combined therapy. Of note, a co-mutation in KRAS may predict lack of response to HER2 directed therapy in HER2 amplified colorectal cancer[50], and gastric cancer[51] although this may not be the case in pancreatic cancer, and it is conceivable that the magnitude of amplification in our patient led to a dependence and oncogenic addition to the HER2 pathway.

Multi-disciplinary collaboration informed a multi-modality treatment strategy, combining surgery, radiation, checkpoint inhibition, personalized vaccine, and anti-HER2 drug antibody conjugate. These treatments were given in a partially concurrent manner to leverage additive benefits observed in pre-clinical and early clinical settings and were staggered to mitigate toxicity. Trastuzumab deruxtecan combined with immunotherapy potentiates a strong immune response and acts synergistically with anti-PD-1 antibody treatment to prolong survival in mice[52]. The combination of radiation with immunotherapy may have an abscopal effect to induce immune response to neoantigens, a theory being studied across multiple cancer types [53], showing activity in colorectal cancer[54] and anecdotal evidence in pancreatic cancer[55]. Combination vaccine therapy with checkpoint inhibition indicates that PD-1 blockade increases CD8 positive effector T cells and prolongs mouse survival compared to vaccine therapy alone[56]. Another preclinical study

combining a neoantigen vaccine with checkpoint inhibition in mice demonstrated prolonged survival compared to vaccine or checkpoint therapy alone[57].

While our organoid modeling was effective for understanding tumor cell-autonomous HER2 response, it did not allow evaluation of the ALI organoid tumor immune cellular compartment, which does not persist long-term; immunotherapy was not a therapeutic consideration at the time of the initial biopsy and organoid generation. However, acute evaluation of checkpoint inhibition within ALI tumor cultures is feasible within the first several weeks of culture and can be considered for future cases[29,58] Also of note, the initial therapy with the immunomodulator agent indoximod, which elicited a partial response, may have primed the subsequent response to checkpoint inhibition. While the phase II trial of the indoximod-containing regimen received by the patient failed to meet its primary endpoint[59], exploratory analyses showed that responders had increased intra-tumoral CD8 density compared to non-responders (p=0.30). The patient was prescribed hydroxychloroquine based on data suggesting an important role of autophagy in regulating MHC-I mediated immunogenicity in PDAC[60], but this was stopped due to intolerance. Lastly, functional assessment of the patient's personalized DNA neoepitope vaccine demonstrated that her T cells were activated against cancer-specific epitopes, thus providing evidence that the vaccine is now contributing at least partially to response and maintenance of remission.

An overall survival advantage for biomarker-directed therapy in PDAC has yet to be demonstrated in a prospective, randomized trial. Nevertheless, several findings suggest that a subset of PDAC patients with targetable alterations are likely to achieve benefit from biomarker-matched therapy. For example, a retrospective, non-randomized study involving PDAC patients eligible for biomarker-matched therapy based on having microsatellite instability, DNA repair gene mutations, or other mutations, had impressive survival as compared to historical averages of unselected PDAC patients[61]. Additionally, long duration of response to olaparib has been observed in patients with germline BRCA mutations[44]. Among the 5-10% of PDAC patients who lack RAS mutations, an enrichment of HER2 mutations, other targetable gene mutations, and microsatellite instability are observed[62]. NCCN guidelines currently recommend that PDAC patients with advanced disease undergo tumor panel gene profiling, including HER2 mutations, and mismatch repair assessment, but do not explicitly recommend HER2 IHC or amplification testing. Anecdotal evidence of exceptional cases may help identify strategies that correlate patient attributes or tumor biomarkers with predictive value in improving outcomes. Collaborative, multi-disciplinary trials combining radiotherapy, immunotherapy, and targeted therapy, may exploit tumor vulnerabilities to guide PDAC precision therapy as exemplified by the current patient.

Acknowledgements

The investigators are indebted to our patient for the permission to publish her clinical story. Informed consent to publish information and/or images from the patient. We appreciate guidance from Maurizio Scaltriti for several organoid analyses. Drs. Sunil Hingorani, Andrew Hendifar, and Ted Hong provided valuable clinical insight. We are grateful to Kevin White, Greg Call, Nike Beaubier, and Amber Solari, at Tempus for sharing HER2 distribution data for research use. We are grateful for support from the NIH (U01CA217851, U54CA224081, R01CA2515143), Seed Grant from the Stanford Cancer Institute, NIH NCI Award (U01CA248235), and V Scholar Award from the V Foundation for Cancer Research (V2018-007).

References

1. Howlader N. SEER Cancer Statistics Review, 1975-2018. Published 2021. https://seer.cancer.gov/csr/1975_2018/
2. Iqbal N, Iqbal N. Human Epidermal Growth Factor Receptor 2 (HER2) in Cancers: Overexpression and Therapeutic Implications. *Mol Biol Int*. 2014;2014:1-9. doi:10.1155/2014/852748
3. Hofmann M, Stoss O, Shi D, et al. Assessment of a HER2 scoring system for gastric cancer: results from a validation study. *Histopathology*. 2008;52(7):797-805. doi:10.1111/j.1365-2559.2008.03028.x
4. Chou A, Waddell N, Cowley MJ, et al. Clinical and molecular characterization of HER2 amplified-pancreatic cancer. *Genome Med*. 2013;5(8):1. doi:10.1186/gm482
5. Stoecklein NH, Luebke AM, Erbersdobler A, et al. Copy number of chromosome 17 but not HER2 amplification predicts clinical outcome of patients with pancreatic ductal adenocarcinoma. *J Clin Oncol*. 2004;22(23):4685-4693. doi:10.1200/JCO.2004.05.142
6. Komoto M, Nakata B, Amano R, et al. HER2 overexpression correlates with survival after curative resection of pancreatic cancer. *Cancer Sci*. 2009;100(7):1243-1247. doi:10.1111/j.1349-7006.2009.01176.x
7. Sapino A, Goia M, Recupero D, Marchiò C. Current challenges for HER2 testing in diagnostic pathology: State of the art and controversial issues. *Front Oncol*. 2013;3 MAY(May):1-9. doi:10.3389/fonc.2013.00129
8. Aumayr K, Soleiman A, Sahora K, et al. HER2 gene amplification and protein expression in pancreatic ductal adenocarcinomas. *Appl Immunohistochem Mol Morphol*. 2014;22(2):146-152. doi:10.1097/PAI.0b013e31828dc392
9. Büchler P, Reber HA, Büchler MC, et al. Therapy for Pancreatic Cancer with a Recombinant Humanized Anti-HER2 Antibody (Herceptin). *J Gastrointest Surg*. 2001;5(2):139-146. doi:10.1016/S1091-255X(01)80025-1
10. Kimura K, Sawada T, Komatsu M, et al. Antitumor effect of trastuzumab for pancreatic cancer with high HER-2 expression and enhancement of effect by combined therapy with gemcitabine. *Clin Cancer Res*. 2006;12(16):4925-4932. doi:10.1158/1078-0432.CCR-06-0544
11. Saeki H, Yanoma S, Takemiya S, et al. Antitumor activity of a combination of trastuzumab (Herceptin) and oral fluoropyrimidine S-1 on human epidermal growth factor receptor 2-overexpressing pancreatic cancer. *Oncol Rep*. 2007;18(2):433-439. doi:10.3892/or.18.2.433
12. Kato Y, Ohishi T, Sano M, et al. H2Mab-19 Anti-Human Epidermal Growth Factor Receptor 2 Monoclonal Antibody Therapy Exerts Antitumor Activity in Pancreatic Cancer Xenograft Models. *Monoclon Antib Immunodiagn Immunother*. 2020;39(3):61-65. doi:10.1089/mab.2020.0011
13. Safran H, Iannitti D, Ramanathan R, et al. Herceptin and gemcitabine for metastatic pancreatic cancers that overexpress HER-2/neu. *Cancer Invest*. 2004;22(5):706-712. doi:10.1081/CNV-200032974
14. Harder J, Ihorst G, Heinemann V, et al. Multicentre phase II trial of trastuzumab and capecitabine in patients with HER2 overexpressing metastatic pancreatic cancer. *Br J Cancer*. 2012;106(6):1033-1038. doi:10.1038/bjc.2012.18
15. Assenat E, Mineur L, Mollevi C, et al. Phase II study evaluating the association of gemcitabine, trastuzumab and erlotinib as first-line treatment in patients with metastatic pancreatic adenocarcinoma (GATE 1). *Int J Cancer*. 2021;148(3):682-691. doi:10.1002/ijc.33225
16. Sleijfer S, Bogaerts J, Siu LL. Designing transformative clinical trials in the cancer

genome era. *J Clin Oncol Off J Am Soc Clin Oncol*. 2013;31(15):1834-1841. doi:10.1200/JCO.2012.45.3639

17. Bang Y-J, Van Cutsem E, Feyereislova A, et al. Trastuzumab in combination with chemotherapy versus chemotherapy alone for treatment of HER2-positive advanced gastric or gastro-oesophageal junction cancer (ToGA): a phase 3, open-label, randomised controlled trial. *Lancet (London, England)*. 2010;376(9742):687-697. doi:10.1016/S0140-6736(10)61121-X
18. Shitara K, Bang Y-J, Iwasa S, et al. Trastuzumab Deruxtecan in Previously Treated HER2-Positive Gastric Cancer. *N Engl J Med*. 2020;382(25):2419-2430. doi:10.1056/NEJMoa2004413
19. Soares KC, Zheng L, Edil B, Jaffee EM. Vaccines for pancreatic cancer. *Cancer J (United States)*. 2012;18(6):642-652. doi:10.1097/PPO.0b013e3182756903
20. Mucciolo G, Roux C, Scagliotti A, Brugiapaglia S, Novelli F, Cappello P. The dark side of immunotherapy: pancreatic cancer. *Cancer Drug Resist*. Published online 2020:491-520. doi:10.20517/cdr.2020.13
21. Henriksen A, Dyhl-Polk A, Chen I, Nielsen D. Checkpoint inhibitors in pancreatic cancer. *Cancer Treat Rev*. 2019;78(March):17-30. doi:10.1016/j.ctrv.2019.06.005
22. Wainberg ZA, Hochster HS, Kim EJ, et al. Open-label, Phase I Study of Nivolumab Combined with nab-Paclitaxel Plus Gemcitabine in Advanced Pancreatic Cancer. *Clin cancer Res an Off J Am Assoc Cancer Res*. 2020;26(18):4814-4822. doi:10.1158/1078-0432.CCR-20-0099
23. Clinicaltrials.gov. NCT04161755. Published 2021. https://clinicaltrials.gov/ct2/show/NCT04161755
24. NCI. Clinical Trials Using GVAX Pancreatic Cancer Vaccine. Published 2021. https://www.cancer.gov/about-cancer/treatment/clinical-trials/intervention/gvax-pancreatic-cancer-vaccine
25. MERCK. FDA Approves Merck's KEYTRUDA® (pembrolizumab) Combined With Trastuzumab and Chemotherapy as First-line Treatment in Locally Advanced Unresectable or Metastatic HER2-Positive Gastric or Gastroesophageal Junction Adenocarcinoma. Published 2021. https://www.merck.com/news/fda-approves-mercks-keytruda-pembrolizumab-combined-with-trastuzumab-and-chemotherapy-as-first-line-treatment-in-locally-advanced-unresectable-or-metastatic-her2-positive-gastric-or-g/
26. Lo Y-H, Karlsson K, Kuo CJ. Applications of organoids for cancer biology and precision medicine. *Nat Cancer*. 2020;1(8):761-773. doi:10.1038/s43018-020-0102-y
27. Baker LA, Tiriac H, Clevers H, Tuveson DA. Modeling pancreatic cancer with organoids. *Trends in cancer*. 2016;2(4):176-190. doi:10.1016/j.trecan.2016.03.004
28. Boj SF, Hwang C-I, Baker LA, et al. Organoid models of human and mouse ductal pancreatic cancer. *Cell*. 2015;160(1-2):324-338. doi:10.1016/j.cell.2014.12.021
29. Neal JT, Li X, Zhu J, et al. Organoid Modeling of the Tumor Immune Microenvironment. *Cell*. 2018;175(7):1972-1988.e16. doi:10.1016/j.cell.2018.11.021
30. Tiriac H, Belleau P, Engle DD, et al. Organoid profiling identifies common responders to chemotherapy in pancreatic cancer. *Cancer Discov*. 2018;8(9):1112-1129. doi:10.1158/2159-8290.CD-18-0349
31. Driehuis E, Van Hoeck A, Moore K, et al. Pancreatic cancer organoids recapitulate disease and allow personalized drug screening. *Proc Natl Acad Sci U S A*. 2019;116(52):26580-26590. doi:10.1073/pnas.1911273116
32. Patel TH, Cecchini M. Targeted Therapies in Advanced Gastric Cancer. *Curr Treat Options Oncol*. 2020;21(9):70. doi:10.1007/s11864-020-00774-4
33. Fox E, Oliver T, Rowe M, et al. Indoximod: An Immunometabolic Adjuvant That Empowers T Cell Activity in Cancer. *Front Oncol*. 2018;8:370. doi:10.3389/fonc.2018.00370

34. Clinicaltrials.gov. Study of IDO Inhibitor in Combination With Gemcitabine and Nab-Paclitaxel in Patients With Metastatic Pancreatic Cancer. Published 2021. https://clinicaltrials.gov/ct2/show/NCT02077881
35. Clinicaltrials.gov. TAPUR: Testing the Use of Food and Drug Administration (FDA) Approved Drugs That Target a Specific Abnormality in a Tumor Gene in People With Advanced Stage Cancer (TAPUR). Published 2021. https://clinicaltrials.gov/ct2/show/NCT02693535
36. Li L, Zhang X, Wang X, et al. Optimized polyepitope neoantigen DNA vaccines elicit neoantigen-specific immune responses in preclinical models and in clinical translation. *Genome Med*. 2021;13(1):56. doi:10.1186/s13073-021-00872-4
37. Clinicaltrials.gov. Chemotherapy, Neoantigen DNA Vaccine in Pancreatic Cancer Patients Following Surgical Resection and Adjuvant. Published 2021. https://clinicaltrials.gov/ct2/show/NCT03122106
38. Parikh A, Wo JY-L, Ryan DP, et al. A phase II study of ipilimumab and nivolumab with radiation in metastatic pancreatic adenocarcinoma. *J Clin Oncol*. 2019;37(4_suppl):391. doi:10.1200/JCO.2019.37.4_suppl.391
39. Palma DA, Olson R, Harrow S, et al. Stereotactic Ablative Radiotherapy for the Comprehensive Treatment of Oligometastatic Cancers: Long-Term Results of the SABR-COMET Phase II Randomized Trial. *J Clin Oncol*. 2020;38(25):2830-2838. doi:10.1200/JCO.20.00818
40. An E, Ock C-Y, Kim T-Y, et al. Quantitative proteomic analysis of HER2 expression in the selection of gastric cancer patients for trastuzumab treatment. *Ann Oncol Off J Eur Soc Med Oncol*. 2017;28(1):110-115. doi:10.1093/annonc/mdw442
41. Conroy T, Desseigne F, Ychou M, et al. FOLFIRINOX versus Gemcitabine for Metastatic Pancreatic Cancer. *N Engl J Med*. 2011;364(19):1817-1825. doi:10.1056/nejmoa1011923
42. Vogel A, Römmler-Zehrer J, Li JS, McGovern D, Romano A, Stahl M. Efficacy and safety profile of nab-paclitaxel plus gemcitabine in patients with metastatic pancreatic cancer treated to disease progression: a subanalysis from a phase 3 trial (MPACT). *BMC Cancer*. 2016;16(1):817. doi:10.1186/s12885-016-2798-8
43. Wang-Gillam A, Hubner RA, Siveke JT, et al. NAPOLI-1 phase 3 study of liposomal irinotecan in metastatic pancreatic cancer: Final overall survival analysis and characteristics of long-term survivors. *Eur J Cancer*. 2019;108:78-87. doi:10.1016/j.ejca.2018.12.007
44. Golan T, Hammel P, Reni M, et al. Maintenance Olaparib for Germline BRCA-Mutated Metastatic Pancreatic Cancer. *N Engl J Med*. 2019;381(4):317-327. doi:10.1056/NEJMoa1903387
45. Palle J, Tougeron D, Pozet A, et al. Trastuzumab beyond progression in patients with HER2-positive advanced gastric adenocarcinoma: a multicenter AGEO study. *Oncotarget*. 2017;8(60):101383-101393. doi:10.18632/oncotarget.20711
46. Antolín S, García-Caballero L, Reboredo C, et al. Is there a correlation between HER2 gene amplification level and response to neoadjuvant treatment with trastuzumab and chemotherapy in HER2-positive breast cancer? *Virchows Arch*. Published online May 2021. doi:10.1007/s00428-021-03104-7
47. Gustavson M. Abstract PD6-01: Novel approach to HER2 quantification: Digital pathology coupled with AI-based image and data analysis delivers objective and quantitative HER2 expression analysis for enrichment of responders to trastuzumab deruxtecan (T-DXd; DS-8201), s. Published 2021. https://cancerres.aacrjournals.org/content/81/4_Supplement/PD6-01
48. Makiyama A, Sukawa Y, Kashiwada T, et al. Randomized, Phase II Study of Trastuzumab Beyond Progression in Patients With HER2-Positive Advanced Gastric or Gastroesophageal Junction Cancer: WJOG7112G (T-ACT Study). *J Clin Oncol Off J Am*

Soc Clin Oncol. 2020;38(17):1919-1927. doi:10.1200/JCO.19.03077

49. Seo S, Ryu M-H, Park YS, et al. Loss of HER2 positivity after anti-HER2 chemotherapy in HER2-positive gastric cancer patients: results of the GASTric cancer HER2 reassessment study 3 (GASTHER3). *Gastric cancer Off J Int Gastric Cancer Assoc Japanese Gastric Cancer Assoc*. 2019;22(3):527-535. doi:10.1007/s10120-018-0891-1
50. Siena S, Sartore-Bianchi A, Marsoni S, et al. Targeting the human epidermal growth factor receptor 2 (HER2) oncogene in colorectal cancer. *Ann Oncol Off J Eur Soc Med Oncol*. 2018;29(5):1108-1119. doi:10.1093/annonc/mdy100
51. Pietrantonio F, Fucà G, Morano F, et al. Biomarkers of Primary Resistance to Trastuzumab in HER2-Positive Metastatic Gastric Cancer Patients: the AMNESIA Case-Control Study. *Clin cancer Res an Off J Am Assoc Cancer Res*. 2018;24(5):1082-1089. doi:10.1158/1078-0432.CCR-17-2781
52. Iwata TN, Ishii C, Ishida S, Ogitani Y, Wada T, Agatsuma T. A HER2-Targeting Antibody-Drug Conjugate, Trastuzumab Deruxtecan (DS-8201a), Enhances Antitumor Immunity in a Mouse Model. *Mol Cancer Ther*. 2018;17(7):1494-1503. doi:10.1158/1535-7163.MCT-17-0749
53. Gajiwala S, Torgeson A, Garrido-Laguna I, Kinsey C, Lloyd S. Combination immunotherapy and radiation therapy strategies for pancreatic cancer-targeting multiple steps in the cancer immunity cycle. *J Gastrointest Oncol*. 2018;9(6):1014-1026. doi:10.21037/jgo.2018.05.16
54. Parikh A. A phase II study of ipilimumab and nivolumab with radiation in microsatellite stable (MSS) metastatic colorectal adenocarcinoma (mCRC). Published 2019. https://ascopubs.org/doi/abs/10.1200/JCO.2019.37.15_suppl.3514
55. Lee Y-H, Yu C-F, Yang Y-C, Hong J-H, Chiang C-S. Ablative Radiotherapy Reprograms the Tumor Microenvironment of a Pancreatic Tumor in Favoring the Immune Checkpoint Blockade Therapy. *Int J Mol Sci*. 2021;22(4). doi:10.3390/ijms22042091
56. Soares KC, Rucki AA, Wu AA, et al. PD-1/PD-L1 blockade together with vaccine therapy facilitates effector T-cell infiltration into pancreatic tumors. *J Immunother*. 2015;38(1):1-11. doi:10.1097/CJI.0000000000000062
57. Kinkead HL, Hopkins A, Lutz E, et al. Combining STING-based neoantigen-targeted vaccine with checkpoint modulators enhances antitumor immunity in murine pancreatic cancer. *JCI insight*. 2018;3(20). doi:10.1172/jci.insight.122857
58. Yuki K, Cheng N, Nakano M, Kuo CJ. Organoid Models of Tumor Immunology. *Trends Immunol*. 2020;41(8):652-664. doi:10.1016/j.it.2020.06.010
59. Bahary N. Phase 2 trial of the IDO pathway inhibitor indoximod plus gemcitabine / nab-paclitaxel for the treatment of patients with metastatic pancreas cancer. Published 2018. https://ascopubs.org/doi/abs/10.1200/JCO.2018.36.15_suppl.4015
60. Yamamoto K, Venida A, Yano J, et al. Autophagy promotes immune evasion of pancreatic cancer by degrading MHC-I. *Nature*. 2020;581(7806):100-105. doi:10.1038/s41586-020-2229-5
61. Pishvaian MJ, Blais EM, Brody JR, et al. Overall survival in patients with pancreatic cancer receiving matched therapies following molecular profiling: a retrospective analysis of the Know Your Tumor registry trial. *Lancet Oncol*. 2020;21(4):508-518. doi:10.1016/S1470-2045(20)30074-7
62. Philip PA. Enrichment of alterations in targetable molecular pathways in KRAS wild-type (WT) pancreatic cancer (PC). Published 2020. https://ascopubs.org/doi/10.1200/JCO.2020.38.15_suppl.4629

Figures

See PowerPoint

Tables

Table 1: Molecular Profiling

Molecular profiling results for the patient's specimens and derived organoids. HER2 amplifications were detected in all tissues assessed. *Pathogenic Missense* and *Structural Variants* were derived from NGS analysis, while variants of uncertain significance are not listed. The mutations detected in the patient's surgical specimens were also detected in the organoid. Tempus copy number variation data were provided for intent of research use only. TMB = tumor mutation burden (based the number of non-synonymous mutations per megabase); PD-L1 expression was assessed using the IHC 22C3 assay. Mutation values are presented in minor allele frequency (%). NR = not reported.

Biomarker Type	**Collection Date**	August 2017	August 2017	November 2018	November 2018	March 2020	March 2020
	Tissue Type	Surgical specimen	Surgical specimen	Surgical specimen	Organoid	Biopsy specimen	Biopsy specimen
	Sequencing Assay	Tempus xT	Tempus xE	Tempus xE	STAMP	Tempus xT	Tempus xE
Pathogenic Missense	TP53 R342*	56.8	41.4	67.7	99.8	21.3	24.7
	KRAS G12D	57.7	35.3	37.3	54.7	9.6	19.4
	NF1 R1362*	4.56	NR	2.2	6.4	NR	NR
Structural Variants	HER2	>=20 copies	>=20 copies	>=20 copies	22.8 copies	>=20 copies	>=20 copies
	TOP2A	>=20 copies	19 copies	12 copies	NR	NR	9 copies
	CDK12	NR	NR	>=20 copies	NR	>=20 copies	>=20 copies
	MYC	amplification	amplification	NR	NR	NR	NR
	FLT3	amplification	NR	NR	NR	NR	NR
	MITF	amplification	NR	NR	NR	NR	NR
	NF1	amplification	NR	NR	NR	NR	NR
	PTP4A3	NR	amplification	NR	NR	NR	NR
	SMAD4	deletion	deletion	NR	0.46 copies	NR	NR
	RARA	NR	NR	NR	NR	NR	9 copies
	TP53	loss of heterozygosity	loss of heterozygosity	loss of heterozygosity	NR	NR	NR
Immune Biomarker	PD-L1	positive (2%)	not performed	negative (<1%)	not performed	negative (<1%)	not performed
	TMB	0.85	0.8	2.1	not performed	3.2	0.4
HER2	IHC (Stanford)	Not performed		3+	3+	3+	
	RNA Sequencing (Tempus)	95+%		99+%	not performed	99.7+%	
	Mass Spectrometry (mProbe)	1870 attomol/ microgram		5895 attomol/ microgram	5048 attomol/ microgram	quantity not sufficient	

Figure Legends

Figure 1: Clinical Timeline
This clinical timeline depicts the interventions delivered and the tumor burden as assessed by CA 19-9 tumor marker and CT scan. Scan burden was measured by approximating the volume of each tumor lesion using the ellipsoid sphere equation, 4/3 * π * A * B * C, where A, B, and C are the lengths of the three semi-axes (radii) of the ellipsoid. Lesions larger than 2 cm at any timepoint are graphed, as well as the total sum of the volumes of each of the 9 lesions present at any time during the scan. D = debulking. M = Metastasectomy. B = Biopsy. H = hydroxychloroquine. TD = trastuzumab deruxtecan. GnP = gemcitabine and nab-paclitaxel. I = ipilimumab. IN = ipilimumab and nivolumab. N = nivolumab. R = Radiation. ULN = upper limit of normal.

Figure 2: Organoid Generation & Validation
Fresh tumor specimens were minced into small tissue fragments, embedded in a collagen scaffold matrix within an inner transwell, and cultured with direct air exposure above and tissue culture below, contained in an outer dish. Air-liquid interface (ALI) organoids were generated and expanded before being converted into submerged extracellular matrix (BME-2) cultures grown within small domes of matrix beneath tissue culture medium. Organoid validation experiments indicated that the organoid matched the original tissue by histology, had HER2 over-expression, and had a genetic mutations profile concordant with the original tissue. Following confirmation of fidelity, the organoids were distributed to several collaborators for additional study as submerged BME-2 organoids.

Figure 3: Organoid Analyses
(A) Western blot analysis of patient-derived pancreatic organoids incubated with neratinib (100 nM) or T-DXd (25 µg/mL) or DMSO as control for 6 days. Actin was used as loading control. The numbers represent the amount of total and phospho-HER2 normalized on Actin and relative to Control. (B) Patient-derived pancreatic organoids were incubated with neratinib (100 nM) or T-DXd (25 µg/mL) or DMSO as control for 6 days. Cell viability was assessed by Cell Titer Glo and shown as percentage relative to control ± SEM (n=3). Statistical analyses were performed using t-test (**, P≤ 0.01; ****, P≤ 0.0001). (C) Patient-derived pancreatic organoids were incubated with neratinib (100 nM) or T-DXd (25 µg/mL) or DMSO as control for 6 days. Annexin V staining was measured by flow cytometry and the percentage of early apoptotic, late apoptotic and necrotic cells was shown as stacked bar graph. (D) *In vivo* efficacy study of a ERBB2-amplified pancreatic PDX treated with neratinib (20 mg/kg, orally every day, 5 days a week) or T-DXd (10 mg/kg, i.v. once every 3 weeks). Measurements show average tumor volumes ± SEM, n=5 mice per group. Comparisons between Vehicle and T-DXd groups were performed using two-way ANOVA test (****, P≤ 0.0001 at the indicated time point). E. Top scoring therapeutics from in vitro drug sensitivity testing of organoids as performed using the PARIS® test by SEngine.

Figure 4: Neoantigen DNA vaccine induces CD4 and CD8 neoantigen-specific T cell responses
(A) Schematic outlining the design, manufacture, administration, and immune monitoring of the neoantigen DNA vaccine. DNA was extracted from both tumor tissue and patient PBMC, while RNA was extracted from tumor tissue only. Tumor/normal exome sequencing was performed to identify somatic genetic alterations. Tumor RNA sequencing was performed to confirm expression of the genetic alterations. The pVAC-Seq suite of software tools was used to identify and prioritize candidate neoantigens. The neoantigen DNA vaccine was designed and manufactured in an academic GMP facility at WUSM. The neoantigen DNA vaccine was administered using an electroporation device. ELISPOT and intracellular cytokine staining were performed to assess the response to vaccination. (B) PBMC obtained before and after vaccination (week 17) were

stimulated in vitro for 12 days with peptides corresponding to the indicated neoantigens followed by IFNγ ELISPOT assay. Vaccination induced a strong response to neoantigens FOXP3, FAM129C, and ANK2. (C) ELISPOT response to neoantigen ANK2 before and after vaccination. (D, E) Intracellular cytokine staining demonstrates that ANK2-specific CD4 and CD8 T cell responses were induced. (F) The response to FOXP3, FAM129C, and ANK2 persists over time. PBMC from the indicated time points were stimulated in vitro for 12 days with peptides corresponding to the neoantigens included in the neoantigen DNA vaccine followed by IFNγ ELISPOT assay. The bars indicate the average response to FOXP3, FAM129C, and ANK2. None of the other neoantigens induced a consistent response over time. Nonspecific background counts, assessed by incubating cells without peptide during the ELISPOT assay, were subtracted. Cells stimulated without peptide during the 12-day culture are indicated as a negative control (Control).

Figure 1

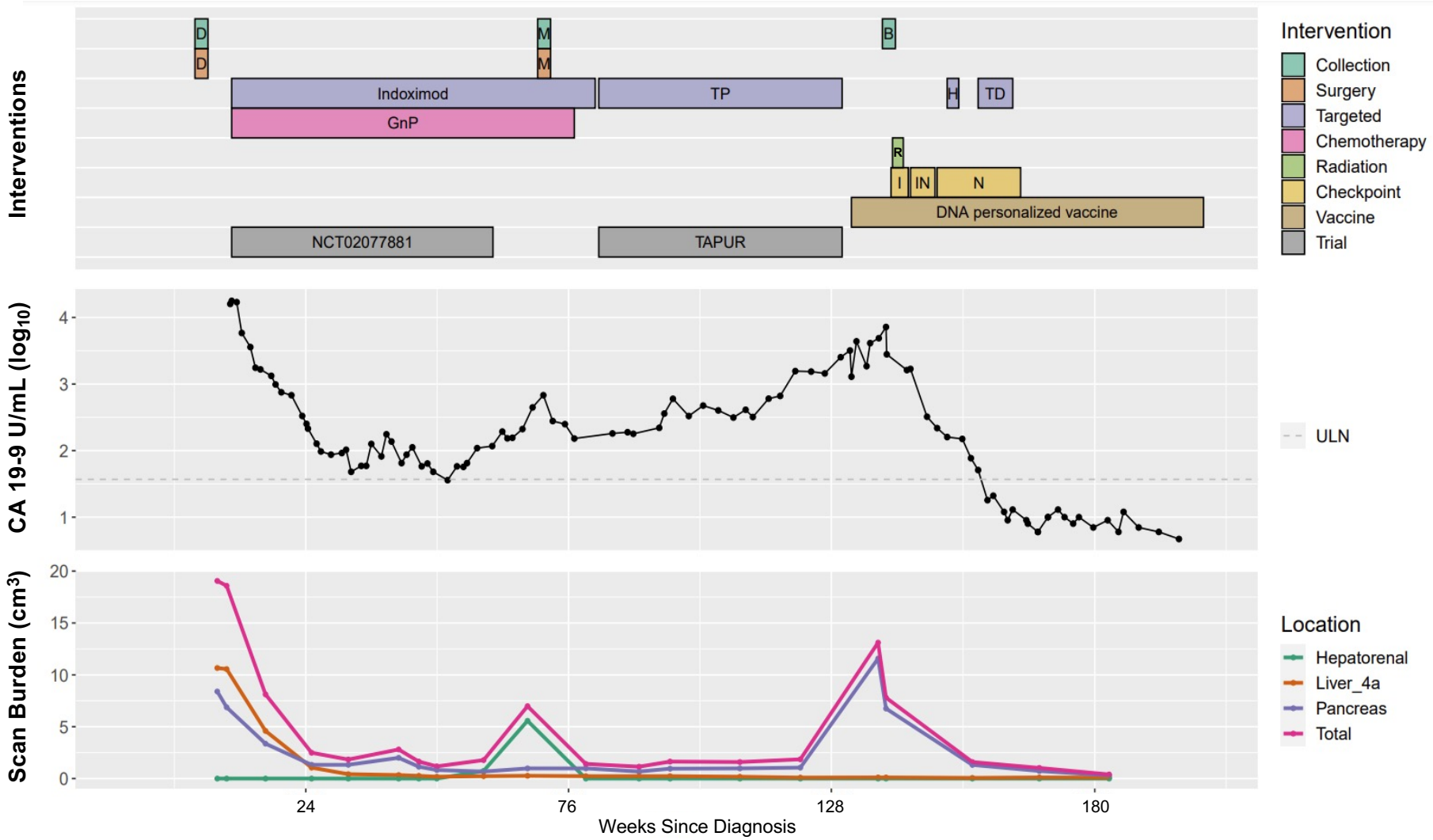
Interventions
D
D
M
M
B
Indoximod
GnP
TP
H
TD
R
I
IN
N
DNA personalized vaccine
NCT02077881
TAPUR
Intervention
Collection
Surgery
Targeted
Chemotherapy
Radiation
Checkpoint
Vaccine
Trial
CA 19-9 U/mL (log10)
4
3
2
1
ULN
Scan Burden (cm3)
20
15
10
5
0
Location
Hepatorenal
Liver_4a
Pancreas
Total
24
76
128
180
Weeks Since Diagnosis

Figure 2

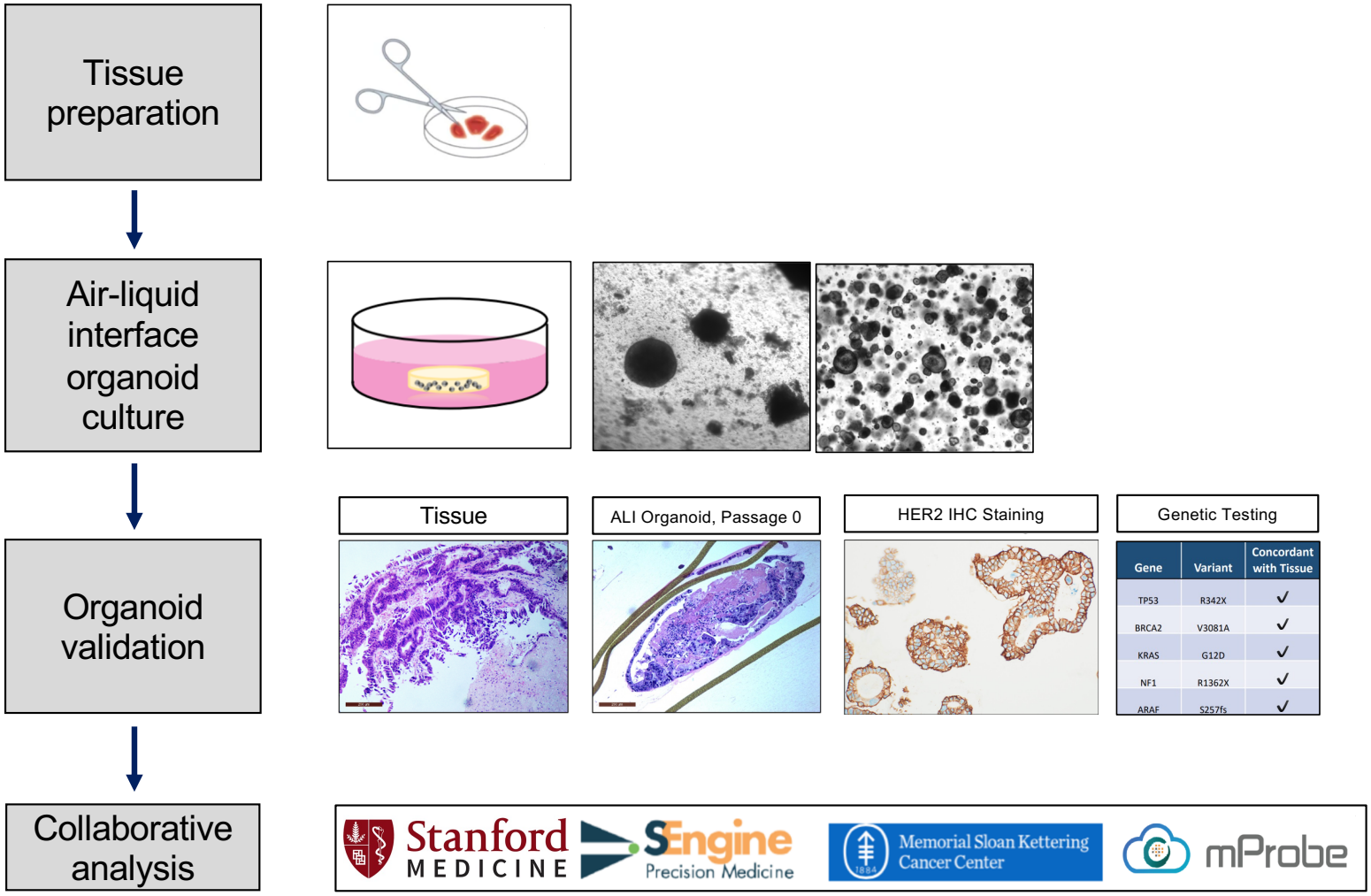
Tissue preparation
Air-liquid interface organoid culture
Organoid validation
Collaborative analysis
Tissue
ALI Organoid, Passage 0
HER2 IHC Staining
Genetic Testing
Gene
Variant
Concordant with Tissue
TP53
R342X
BRCA2
V3081A
KRAS
G12D
NF1
R1362X
ARAF
S257fs
Stanford MEDICINE
SEngine Precision Medicine
Memorial Sloan Kettering Cancer Center
mProbe

Figure 3

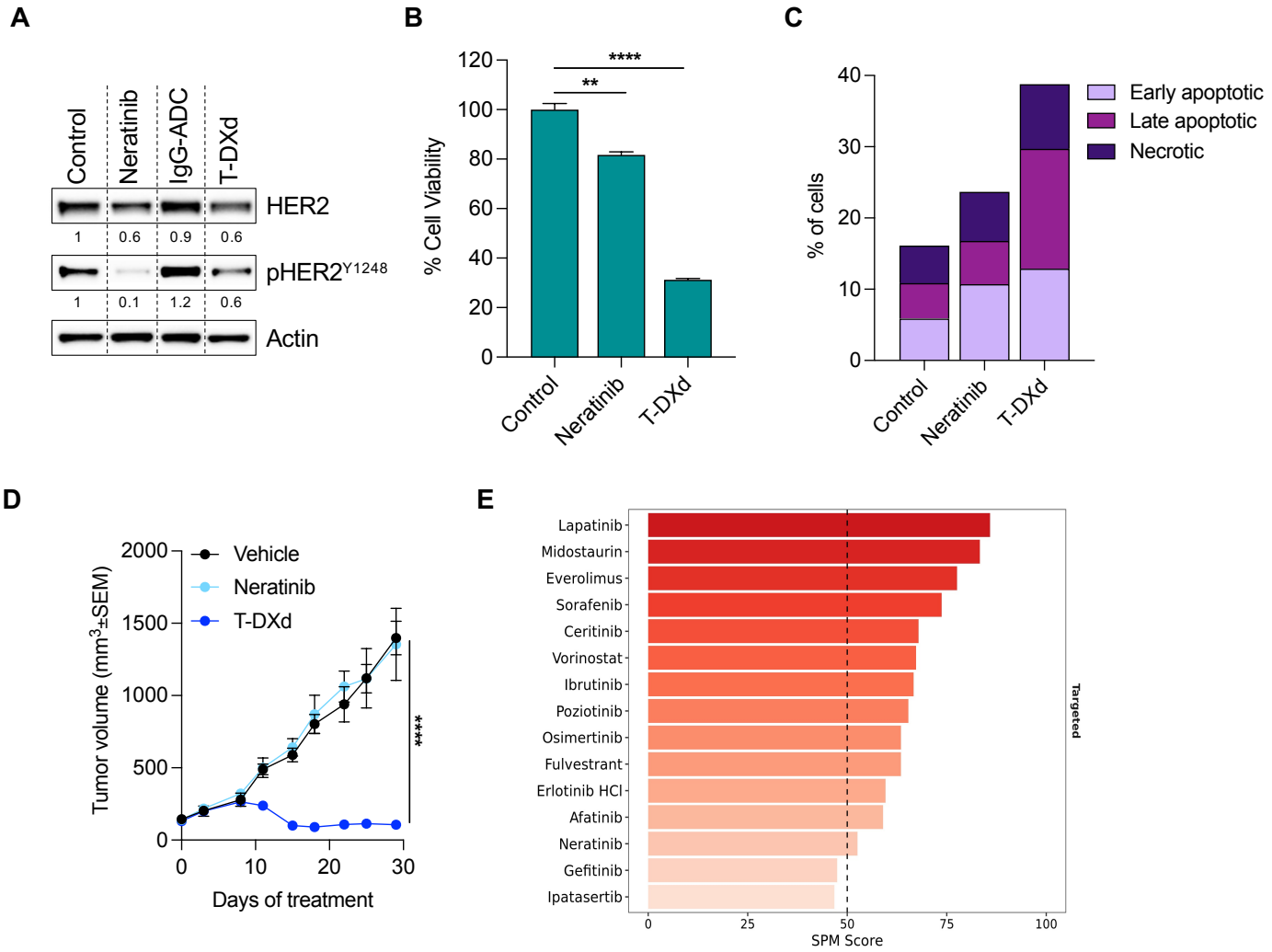
A
Control
Neratinib
IgG-ADC
T-DXd
HER2
1
0.6
0.9
0.6
pHER2Y1248
1
0.1
1.2
0.6
Actin
B
% Cell Viability
****
**
Control
Neratinib
T-DXd
C
% of cells
Early apoptotic
Late apoptotic
Necrotic
Control
Neratinib
T-DXd
D
Tumor volume (mm3±SEM)
Vehicle
Neratinib
T-DXd
****
Days of treatment
E
Lapatinib
Midostaurin
Everolimus
Sorafenib
Ceritinib
Vorinostat
Ibrutinib
Poziotinib
Osimertinib
Fulvestrant
Erlotinib HCl
Afatinib
Neratinib
Gefitinib
Ipatasertib
Targeted
SPM Score

Figure 4

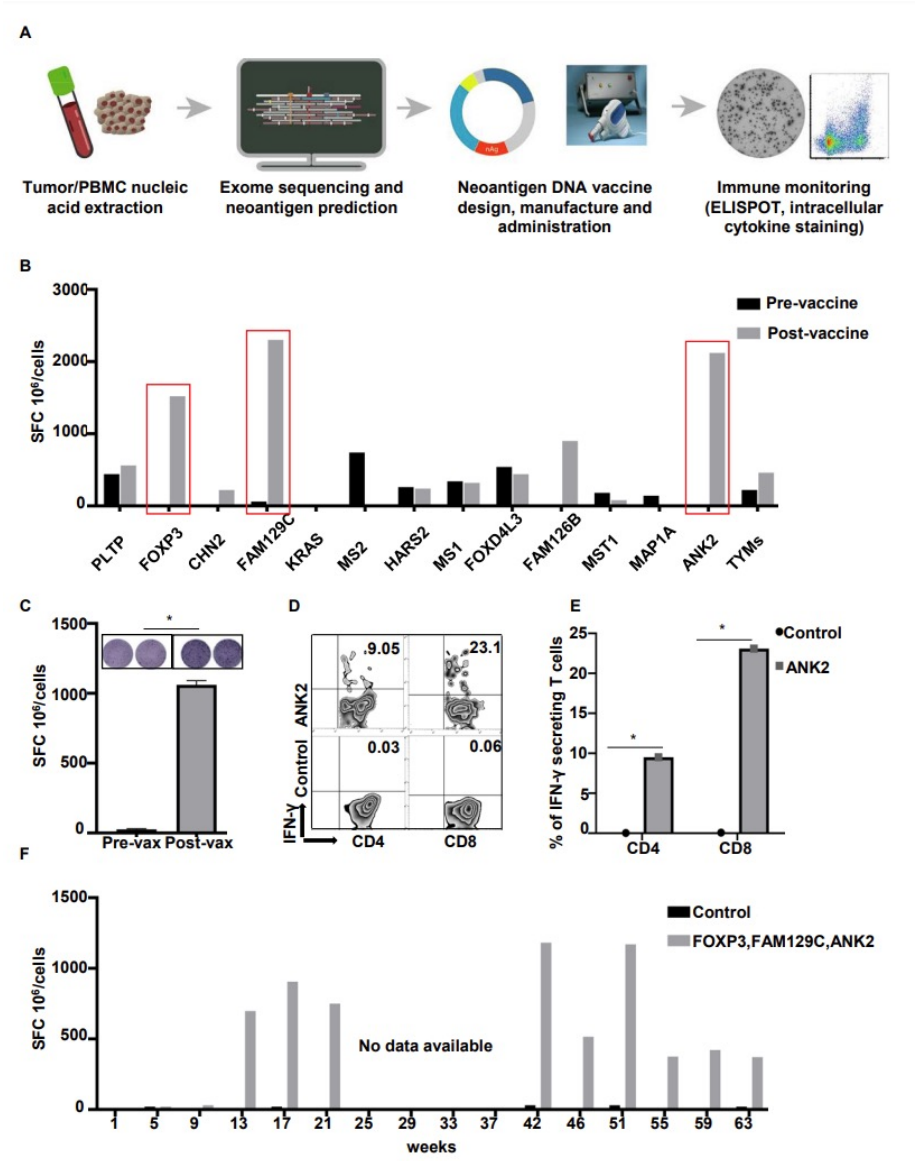
A
Tumor/PBMC nucleic acid extraction
Exome sequencing and neoantigen prediction
Neoantigen DNA vaccine design, manufacture and administration
Immune monitoring (ELISPOT, intracellular cytokine staining)
B
SFC 10⁶/cells
Pre-vaccine
Post-vaccine
PLTP
FOXP3
CHN2
FAM129C
KRAS
MS2
HARS2
MS1
FOXD4L3
FAM126B
MST1
MAP1A
ANK2
TYMs
C
SFC 10⁶/cells
Pre-vax
Post-vax
D
ANK2
Control
IFN-γ
9.05
23.1
0.03
0.06
CD4
CD8
E
% of IFN-γ secreting T cells
Control
ANK2
CD4
CD8
F
SFC 10⁶/cells
Control
FOXP3,FAM129C,ANK2
No data available
weeks

Supplementary Materials

Contents

Organoid Generation 2
Supplementary Figure 1: Confocal Immunofluorescence 2
MSK Studies 3
Western Blot 3
Cell Viability 3
Flow Cytometry 3
Supplementary Figure 2: MSK Flow Cytometry Data: 3
In Vivo Study 4
SEngine Studies 5
Description of the PARIS® Test 5
Supplementary Table 1: SEngine Top Response Drugs 6
Trastuzumab Drug Combination Testing 7
mProbe Studies 8
Personalized Vaccine Therapy 8
Regulatory approval of the neoantigen DNA vaccine 8
Neoantigen DNA vaccine design and manufacture 8
Supplementary Table 2: Neoantigens included in the neoantigen DNA vaccine 8
Vaccine administration 9
ELISPOT assay 9
Flow cytometry 9
Statistics 9
References 10

Organoid Generation

Core biopsy samples were transported to the lab in HypoThermosol ® FRS preservative solution (StemCell Technologies, #07935) on ice. As described previously, the biopsy sample was minced, resuspended in collagen type 1 matrix and transferred into an inner transwell containing a base layer of collagen type 1 matrix (Fujifilm Wako Chemicals, Cellmatrix Type 1-A, #631-00651)[1]. Organoids were generated and maintained in culture using WENR media as described in Neal, et al, 2018. Upon ALI organoid generation, collagen was dissociated using collagenase and organoids dissociated using TrypLE Express (Gibco). Dissociated organoids were resuspended in Cultrex® Reduced Growth Factor Basement Membrane Matrix, Type 2 (BME-2) (R&D Systems) for submerged organoid culture.

Supplementary Figure 1: Confocal Immunofluorescence

Confocal immunofluorescence images from submerged organoids collected 1 hour post-trastuzumab treatment demonstrate the 3D organoid colony. This image confirms trastuzumab localization to cellular membranes in HER-2 expressing organoids.

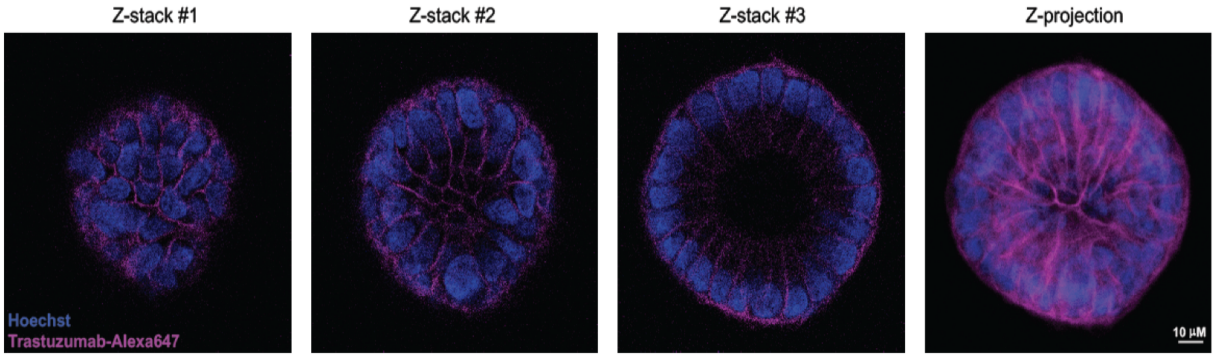

MSK Studies

Western Blot

Organoids were plated into 6-well plates and treated with DMSO, neratinib 100nM or T-DXd 25 μg/mL for 6 days. Corning® Cell Recovery Solution was used to recover organoids cultured on Corning® Matrigel® according to manufacturer's instructions. Total protein lysates (20 μg) were extracted using RIPA buffer and separated on SDS-PAGE gels (NuPAGE 4–12% Bis-Tris Protein Gels, Invitrogen) according to standard methods. Membranes were probed using the following antibodies: anti-total HER2 Rabbit mAb (29D8, Cell Signaling Technology #2165), anti-phospho-HER2 (Tyr1248, Cell Signaling Technology #2247) and anti-β-Actin 13E5 (Cell Signaling Technology #4970). ImageJ was used to quantify western blot band intensity.

Cell Viability

The CellTiter-Glo luminescent cell viability assay was performed on each sample according to the manufacturer's instructions (Promega, G7570). Briefly, organoids were plated in triplicate onto 96-well plates. After an incubation for 24 h, organoids were treated with DMSO, neratinib 100nM or T-DXd 25 μg/mL for 6 days. Organoids were then incubated for 1 hour at 37 degrees Celsius with CellTiter-Glo reagent, and luminescence was measured using a 96-well plate reader. Background luminescence was measured in medium without organoids and subtracted from experimental values.

Flow Cytometry

Organoids were plated in a 12-well plate and cultured in presence of DMSO, neratinib 100nM or T-DXd 25 mg/mL for 6 days. For the apoptosis assessment, cells were collected, resuspended, and analyzed for phosphatidylserine exposure by staining with DAPI and Annexin V APC (550474; BD Bioscience) after incubation with Annexin V binding buffer (556454; BD Pharmingen) according to the manufacturer's instructions. A minimum of 10.000 cells were acquired using FACS CANTO II instrument (BD, Heidelberg,Germany) and data was analyzed using FlowJo v10 software (Tree Star, Ashland, OR).

Supplementary Figure 2: MSK Flow Cytometry Data:

FACS analysis of PDAC-35T organoids after 6-days treatment. Neratinib = panHER irreversible inhibitor, T-DM1 = anti-HER2 ADC, DS-8201a = anti-HER2 ADC, U3-1402 = anti-HER3 ADC.

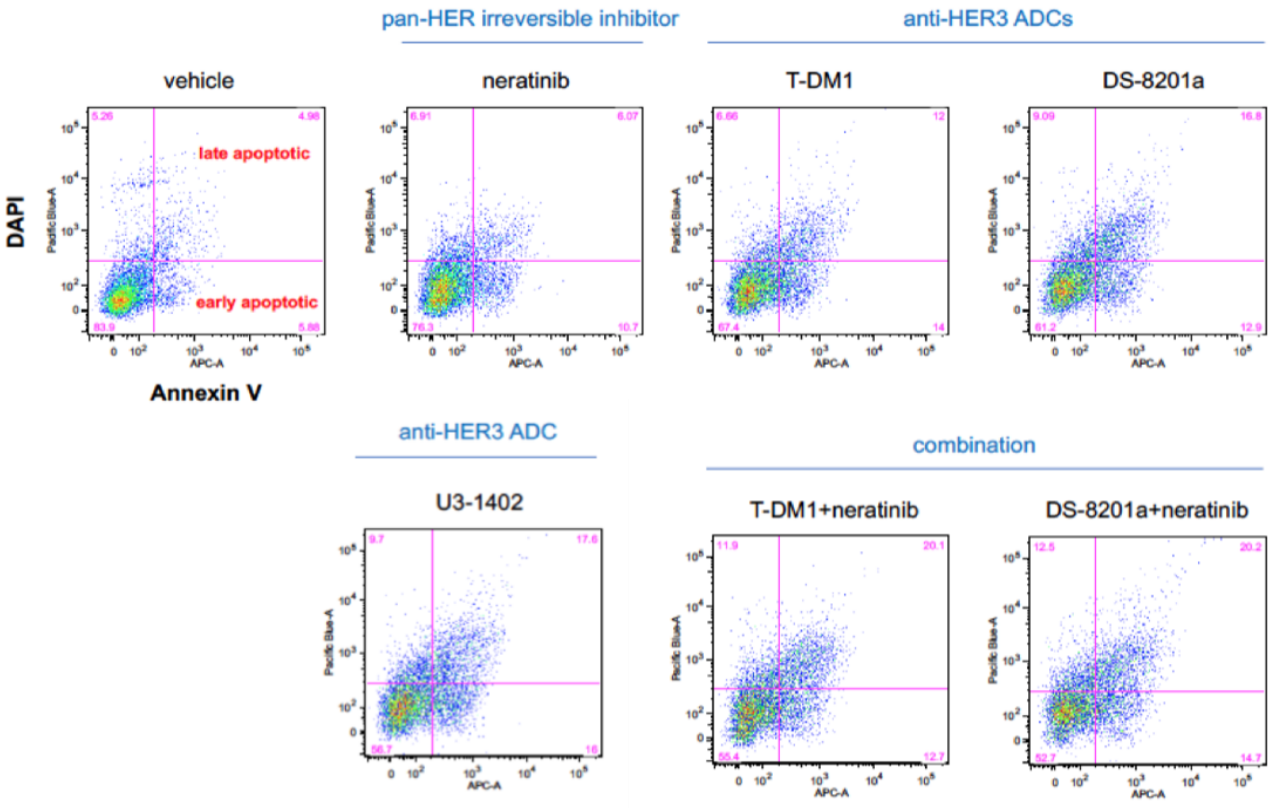

In Vivo Study

The ERBB2-amplified pancreatic patient-derived xenograft (PDX) was generated as follows: 6-week-old NOD SCID gamma female mice were implanted subcutaneously with specimens freshly collected from a patient at MSK under an MSK-approved IRB bio-specimen protocol #06-107. Tumors developed within 2 to 4 months and were expanded into additional mice by serial transplantation. At this point, the PDX was subjected to high-coverage NGS with the MSK-IMPACT assay. For the efficacy study, treatment was started when tumor volumes reached approximately 150 mm^3. Xenografts were randomized and dosed with neratinib (20 mg/kg, orally 5 days a week), T-DXd (10 mg/kg, intravenously once every 3 weeks), or vehicle as control (saline, orally 5 days a week). Mice were observed daily throughout the treatment period for signs of toxicity. Tumors were measured twice weekly using calipers, and tumor volume was calculated using the formula length × $width^2$ × 0.52. Body weight was also assessed twice weekly. At the end of each treatment, animals were sacrificed, and tumors were collected for biochemistry and histology analysis. Mice were cared for in accordance with guidelines approved by the MSK Institutional Animal Care and Use Committee and Research Animal Resource Center. Five (5) mice per group were included in the experiment.

SEngine Studies

SEngine Precision Medicine (SPM) received patient-derived organoids (PDO) from Dr. Calvin Kuo's laboratory, which were derived from a case of pancreatic adenocarcinoma (PDAC) with peritoneal metastasis. Organoids were expanded for 4 weeks at SPM and plated for the drug sensitivity CLIA-certified assay, PARIS® Test, measuring drug response across a panel of oncology drugs. For each case, drugs are selected based on the cancer type, genomic knowledge, as well as the SPM knowledge base where available, as well as the doctor's recommendations. The current PARIS test aims to test up to 44 drugs, provided that sufficient material is obtained. At the time this test was performed, the results were ranked with a score from 100 - 1, with drugs that exhibited any degree of sensitivity receiving a score between 100 to 50, generally.

Since 2020, categories have been added to numerical scores and the score has been condensed from 15 to 1. The recent clinical analysis of the scorings system and categories has indicated a strong correlation (~70%) in both the retrospective and prospective setting[2]. Curated categories that characterize drug responses have been added comprising: *Exceptional*, *Good*, *Moderate*, *Low* and None. Only drugs scoring at least *Low* are presented.

The drug panel for this patient consisted of 39 targeted drugs, each tested at 6 dilution points as specified further below covering the following targets and pathways: EGFR & HER2, PARP, ER, MEK, PI3K/AKT/mTOR, FLT3, BET, BCR-ABL/SRC and VEGFR.

The results of the PARIS® assay indicated lapatinib as a top-scoring drug with a categorization of *Exceptional/Good*, borderline between exceptional to good, with the updated scoring system. Lapatinib, a HER2 small molecule inhibitor, is used in the PARIS® Test as a surrogate for HER2-directed therapies such as trastuzumab. This result was in concordance with the presence of high levels of HER2 amplification and overexpression as detected by genomics and IHC clinical tests. In addition, EGFR targeting poziotinib, ibrutinib, osimertinib and erlotinib all showed *Moderate* response. Other top scoring drugs included midostaurin, a multi-kinase inhibitor developed for FLT3 mutant leukemias. Interestingly, also quizartinib, a FLT3 inhibitor, indicated a *Moderate/Low* response. In addition, a *Good* response was detected to Everolimus, and a *Low* response to the AKT inhibitor, ipatasertib, the latter is typical for this class of drugs that are best used as combination therapies. Of note, despite the presence of a KRAS G12D mutation, this case did not demonstrate sensitivity to MAPK inhibitors used as single agents, such as trametinib or cobimetinib.

Description of the PARIS® Test

The PARIS® Test is a high throughput and high complexity CLIA-certified assay applied to cancer specimens grown with specific media and conditions for each cancer type. The media and procedures have been optimized at SPM to promote selection of tumor cells over stroma and other cellular components, such as lymphocytes. For this case, already established organoids were received by Dr. Calvin Kuo's laboratory and expanded using standard conditions for PDAC organoids.

HTS assay: Briefly, the PARIS® Test assay is carried out in 384-well format and drugs are assayed with a 6 point-drug titration spanning generally a range of concentrations, from Log10e-7.5(M) to Log10e-5(M). Depending on the therapeutic range, certain drugs may be tested within a different set of concentrations. Methods pertaining the high-throughput drug sensitivity assay, including drug combination studies, were as described in previous publications[3,4].

Supplementary Table 1: SEngine Top Response Drugs

Table of top-scoring targeted drugs displayed with corresponding targets, maximum observed serum dose (Cmax), and IC50. Drugs are ranked by SPM score, which is a proprietary ranking metric of drug sensitivity that weighs sensitivity and uniqueness of response obtained through the PARIS® Test, on a scale with values from 100 - 1 ranked from the best to the worst for each patient. High numbers (100 - 50) indicate drugs with some degree of response, while a SPM score below 50 generally indicated low to no response. Rank is of guidance but should not be considered the only metric to select drugs as clinical consideration and genomic evidence should be considered for example.

Drug	Target	Cmax	Inhib.Cmax	IC50	SPM	Interpretation
Lapatinib	EGFR, HER2	4.00E-06	91	9.70E-07	85.9	Exceptional/Good
Midostaurin	FLT3, PKCα, PKCβ, PKCγ, Syk, Flk-1, Akt, PKA, c- Kit, FGFR, SRC, PDFRβ, VEGFR1, VEGFR2	1.40E-06	64.3	3.50E-07	83.3	Good
Everolimus	mTORC1	3.90E-08	31.3	1.40E-06	77.6	Good
Sorafenib	VEGFR, PDGFR, Raf	2.10E-05	NA	2.00E-06	73.7	Good
Ceritinib	ALK, IGF-1R, ROS1	1.40E-06	49.4	1.50E-06	67.9	Moderate
Vorinostat	histone deacetylase	2.20E-06	58.6	1.70E-06	67.3	Moderate
Ibrutinib	BTK	8.70E-07	40.9	2.20E-06	66.7	Moderate

Poziotinib	EGFR, HER2, HER4	1.70E-07	57.3	NA	65.4	Moderate
Fulvestrant	selective estrogen receptor degrader	2.10E-08	NA	NA	63.5	Moderate/Low
Osimertinib	EGFR	1.30E-07	24.3	1.50E-06	63.5	Moderate/Low
Erlotinib HCl	EGFR, ALK, JAK2 mutant (JAK2V617F)	5.40E-06	77.8	7.70E-07	59.6	Moderate
Afatinib	EGFR, HER2	3.90E-07	46.1	1.40E-06	59	Low, IC50 is higher than Cmax
Neratinib	EGFR, HER1, HER2, HER4	2.10E-07	33.3	6.30E-07	52.6	Low
Gefitinib	EGFR	3.60E-07	28.8	2.10E-06	47.4	Low
Ipatasertib	pan-AKT	NA	NA	NA	46.8	Low, partial 30% response

Trastuzumab Drug Combination Testing

Subsequently, a drug combination study aiming to identify potential drugs to enhance the effect of trastuzumab was performed as a custom research study. Trastuzumab was titrated onto the PDOs to obtain the IC30 concentration which was determined at 200 ng/ml. This single concentration of trastuzumab was employed as a "sensitizer" against an additional panel of 24 drugs. Results indicated enhanced inhibition of PDO growth with the combination of trastuzumab with the MEK inhibitor cobimetinib. This drug combination testing revealed a "hidden" sensitivity to inhibition of the MAPK pathway, which emerged upon inhibition of the HER2 receptor. This result may be explained by the presence of the KRAS G12D mutation, which generally correlates with a strong response to MEK inhibitors. In addition, the drug combination study showed enhanced growth inhibition by the combination of trastuzumab and adavosertib. The latter targets the cell cycle checkpoint kinase WEE1. The presence of a TP53 stop gain mutation (p.R343) in this specimen may underline the sensitivity of this specimen to adavosertib.

mProbe Studies

Selected reaction monitoring-mass spectrometry (SRM-MS) of 72 biomarkers of the tissue sections from FFPE blocks was conducted as previously described[5,6]. Briefly, two tissue section sections (10µM each) from FFPE blocks were placed on DIRECTOR slides, deparaffinized, and stained with hematoxylin. Tumor areas were marked by board-certified pathologist which was microdissected and solubilized to tryptic fragments as per manufacturer instructions (Expression Pathology, Rockville, MD). Protein concentrations of the tryptic peptides was calculated using microBCA. Stable heavy isotope-labeled internal standard peptides for 72 biomarkers were added to the solution and injected into the mass spectrometer (TSQ Quantiva, ThermoFisher Scientific, San Jose, CA). On-column injection resulted in 5fmol of isotopically labeled internal standard peptide and 1µg of total tumor protein. Data analysis of the 72 biomarkers was conducted using Pinnacle software (Optys Tech, Boston, MA).

Personalized Vaccine Therapy

Regulatory approval of the neoantigen DNA vaccine

The neoantigen DNA vaccine treatment protocol was approved by the Washington University School of Medicine (WUSM) Institutional Review Board, the Institutional Biosafety Committee, and the Food and Drug Administration. Written informed consent was obtained from the patient.

Neoantigen DNA vaccine design and manufacture

DNA from both tumor tissue and peripheral blood mononuclear cells (PBMCs) was extracted using the QIAamp DNA Mini Kit (Qiagen Sciences, Maryland), and RNA was extracted from tumor tissue using the High Pure RNA Paraffin kit (Roche, Indianapolis). DNA and RNA quality and quantity were assessed using a Nanodrop 2000 and a Qubit Fluorometer (Life Technologies, Carlsbad, CA), respectively. Exome sequencing and cDNA-capture sequencing were performed at the McDonnell Genome Institute at WUSM followed by selection and prioritization of candidate neoantigens using the prediction algorithms in the pVAC tools suite of software[7]. The candidate neoantigens were subsequently cloned into a pING plasmid backbone, as previously described[8,9]. In addition, two epitopes derived from mesothelin, a pancreas cancer-associated tumor antigen, mesothelin were included[10–12]. The neoantigen DNA vaccine was manufactured at the Biologic Therapy Core Facility at WUSM. Extensive product release tests were performed to confirm the identity of the plasmid, and the suitability of the plasmid for administration prior to release (Fig 1A).

Supplementary Table 2: Neoantigens included in the neoantigen DNA vaccine

Gene name	Gene mutation	MT-25-mer Seq*	HLA Allele	MT score	WT score	Fold change
PLTP	F220V	EERMVYVAFSEFVFDSAMESYFRAG	HLA-A*26:01	65.1	1451.4	22.3
FOXP3	A349T	AFFRNHPATWKNTIRHNLSLHKCFV	HLA-B*53:01	311.2	506.1	1.6
CHN2	FS.TGA/T	KFIDAAKISNADEAGSRP	HLA-C*04:01	N/A	N/A	N/A
FAM129C	G520R	RGRVLKKFKSDSRLAQRRFIRGWGL	HLA-C*06:02	163.7	5567.6	34
KRAS	G12D	MTEYKLVVVGADGVGKSALTIQLIQ	HLA-A*02:01	338.8	455.7	1.3
MS^{1}2	NA	FMKLRTDAVLPLTVAEVQKLLGPHV	HLA-A*02:01	N/A	N/A	N/A
HARS2	R129C	DLKDQGGELLSLCYDLTVPFARYLA	HLA-A*02:01	35.7	93.5	2.6
MS^{1}1	NA	SCGTPALGSLLFLLFSLGWVQPSRT	HLA-A*02:01	N/A	N/A	N/A
FOXD4L3	P110R	AASEDARQPAKPRYSYIALITMAIL	HLA-C*06:02	102.7	18581.1	180.9

FAM126B	I263M	GQWDLGQEVLDDMIYRAQLELFSQP	HLA-A*02:01	17.1	14.1	0.8
MST1	G143S	TEGLLAPVGACESDYGGPLACFTHN	HLA-B*50:02	470.8	862.8	1.8
MAP1A	R104C	ADNLPGINGLLQCKVAELEEEQSQG	HLA-A*02:01	65	173.8	2.7
ANK2	R2714H	EEKDSESHLAEDHHAVSTEAEDRSY	HLA-A*02:01	46.1	78.5	1.7
TYMS	A191V	MCAWNPRDLPLMVLPPCHALCQFYV	HLA-A*02:01	329.2	1883	5.7

* Amino acids that differ from wildtype sequences are indicated in red. The minimal epitope with the highest predicted affinity is underlined. MS1: Mesothelin

Vaccine administration

The neoantigen DNA vaccine was administered monthly using an integrated electroporation device (TDS-IM system, Ichor Medical Systems, San Diego, CA). At each vaccine time point, the patient received two injections of 2 mg DNA vaccine (4 mg total at each time point). To date, the patient has received 16 months of vaccinations. At each vaccine time point, peripheral blood was drawn and PBMCs were isolated by Ficoll-Paque PLUS (GE Healthcare) density centrifugation and cryopreserved.

ELISPOT assay

IFN-γ ELISpot^{PLUS} Kits (Mabtech, Cincinnati, OH) were used according to the manufacturer's instructions and as detailed below to measure neoantigen-specific immune responses[8,9]. Overlapping synthetic peptides of 15-16 amino acids in length corresponding to the neoantigens included in the neoantigen DNA vaccine were synthesized by LifeTein (Hillsborough, New Jersey, USA). Three peptides overlapping by 11 amino acids were synthesized for each neoantigen included in the vaccine. Synthetic peptides corresponding to the two mesothelin epitopes were also synthesized. Cryopreserved PBMCs were thawed, and typically plated at 2×10^5 per well in duplicate or triplicate followed by 12 days *in vitro* stimulation with pooled peptides. During the 12-day culture, overlapping peptides (2 μM) for two candidate neoantigens were pooled and added to PBMC in the presence of human IL-2 (50 U/mL). After 12 days, lymphocytes were harvested and rested overnight in culture medium without peptides and IL-2. The next day, 10^5 of the rested cells were co-cultured in the ELISpot plate for 20 h with 10^4 of irradiated (3000 Rad) autologous PBMCs pulsed with (or without) peptides (5 μM) corresponding to the neoantigens used in the 12-day cultures. The ELISpot plates were scanned and analyzed on an ImmunoSpot Reader (CTL, Shanker Heights, OH).

Flow cytometry

The following anti-human monoclonal antibodies (mAb) were used for staining: live/dead AF488 (ThermoFisher Scientific, Waltham, MA), CD4-PerCP-Cy5.5 (clone: RPA-T4), CD8-PE (clone: HIT8a), and IFN-gamma-APC (clone B27). All antibodies were purchased from BD Bioscience (San Jose, CA). Samples were acquired on a flow cytometer (BD Biosciences), and data were analyzed using FlowJo software.

Statistics

Data were analyzed using GraphPad Prism 9 software (GraphPad, La Jolla, CA) and presented as mean or the mean ± SEM, where appropriate. The Student *t* test and one-way ANOVA were used to compare between data sets. A $P < 0.05$ was considered statistically significant.

References

1. Neal JT, Li X, Zhu J, et al. Organoid Modeling of the Tumor Immune Microenvironment. *Cell*. 2018;175(7):1972-1988.e16. doi:10.1016/j.cell.2018.11.021

2. Margossian A. A cancer organogram test as a guide for oncology treatments in SOLID tumors: An analysis of 628 tests in 419 patients. Published 2021. https://ascopubs.org/doi/abs/10.1200/JCO.2021.39.15_suppl.2602

3. Pauli C, Hopkins BD, Prandi D, et al. Personalized In Vitro and In Vivo Cancer Models to Guide Precision Medicine. *Cancer Discov*. 2017;7(5):462-477. doi:10.1158/2159-8290.CD-16-1154

4. Lui GYL, Shaw R, Schaub FX, et al. BET, SRC, and BCL2 family inhibitors are synergistic drug combinations with PARP inhibitors in ovarian cancer. *EBioMedicine*. 2020;60:102988. doi:10.1016/j.ebiom.2020.102988

5. Hembrough T, Thyparambil S, Liao W-L, et al. Application of selected reaction monitoring for multiplex quantification of clinically validated biomarkers in formalin-fixed, paraffin-embedded tumor tissue. *J Mol Diagn*. 2013;15(4):454-465. doi:10.1016/j.jmoldx.2013.03.002

6. Catenacci DVT, Liao W-L, Thyparambil S, et al. Absolute quantitation of Met using mass spectrometry for clinical application: assay precision, stability, and correlation with MET gene amplification in FFPE tumor tissue. *PLoS One*. 2014;9(7):e100586. doi:10.1371/journal.pone.0100586

7. Hundal J, Carreno BM, Petti AA, et al. pVAC-Seq: A genome-guided in silico approach to identifying tumor neoantigens. *Genome Med*. 2016;8(1):1-11. doi:10.1186/s13073-016-0264-5

8. Zhang X, Kim S, Hundal J, et al. Breast Cancer Neoantigens Can Induce CD8(+) T-Cell Responses and Antitumor Immunity. *Cancer Immunol Res*. 2017;5(7):516-523. doi:10.1158/2326-6066.CIR-16-0264

9. Li L, Zhang X, Wang X, et al. Optimized polyepitope neoantigen DNA vaccines elicit neoantigen-specific immune responses in preclinical models and in clinical translation. *Genome Med*. 2021;13(1):56. doi:10.1186/s13073-021-00872-4

10. Argani P, Iacobuzio-Donahue C, Ryu B, et al. Mesothelin is overexpressed in the vast majority of ductal adenocarcinomas of the pancreas: identification of a new pancreatic cancer marker by serial analysis of gene expression (SAGE). *Clin cancer Res an Off J Am Assoc Cancer Res*. 2001;7(12):3862-3868.

11. Ordóñez NG. Application of mesothelin immunostaining in tumor diagnosis. *Am J Surg Pathol*. 2003;27(11):1418-1428. doi:10.1097/00000478-200311000-00003

12. Hassan R, Laszik ZG, Lerner M, Raffeld M, Postier R, Brackett D. Mesothelin is overexpressed in pancreaticobiliary adenocarcinomas but not in normal pancreas and chronic pancreatitis. *Am J Clin Pathol*. 2005;124(6):838-845.